Spatially Resolved NMR in Polymer Science

Bernhard Blümich*[1], Peter Blümler[1], Lothar Gasper[1], Andreas Guthausen[1], Volker Göbbels[1], Simone Laukemper-Ostendorf[1], Klaus Unseld[2], Gisela Zimmer[1]

[1]Magnetic Resonance Center MARC, Rheinisch-Westfälische Technische Hochschule, D-52056 Aachen, Germany

[2]Dunlop AG, Dunlopstr. 2, D-63450 Hanau, Germany

SUMMARY: Selected applications of spatially resolved NMR are presented, which demonstrate the use of the method for investigating applied topics relevant to polymer and materials science. Examples are given for imaging of rigid, soft, and fluid matter. They include characterization and interpretation of electrical aging in poly(ethylene), cross-link density at the interface of covulcanized elastomer sheets, and cross-filtration in hollow-fiber filter modules. A novel NMR dectector, the NMR-MOUSE, has been developed for process and quality control by relaxation measurements. Its use for non-destructive determination of the glass-transition temperature by room temperature measurements on elastomer samples is demonstrated.

Introduction

NMR imaging is gaining more and more acceptance as an analytical tool in investigations of applied non-medical issues[1,2]. The method is non-invasive so that functional properties of materials can be imaged, which are being lost by cutting in destructive analysis, and a large variety of contrast parameters become accessible, which allow for visualization of otherwise undetectable features[3]. These arguments clearly apply to the detection and analysis of interfacial layers in rubber covulcanizates, which, in fact, were discovered by NMR imaging[4] and are now being analyzed by a number of different techniques[5]. They are valid also for the characterization of material flow, where NMR provides unique possibilities, because, for example, velocity vector fields of fluids in non-conducting environments can be mapped readily in three dimensions[6,7]. Because NMR is a method of molecular analysis, substantial detailed insight can be obtained into the origins of material change. This point is illustrated by investigating changes in the average morphology of poly(ethylene) from electrical aging leading to the formation of electrical trees[8,9]. Since NMR imaging uses inhomogeneous magnetic fields for spatial localization, and because the measurement of many important contrast parameters does not require homogeneous fields, a new NMR device, the NMR-

 CCC 1022-1360/99/$ 17.50+.50/0

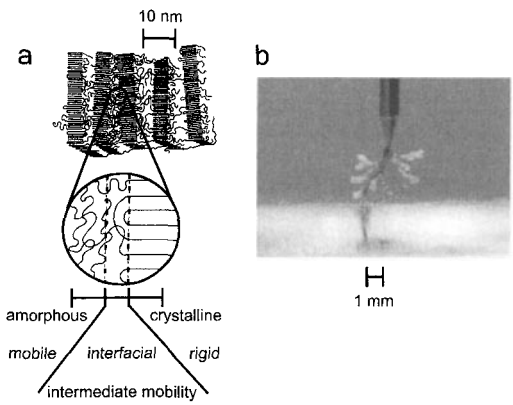

Fig. 1: Semicrystalline structure of poly(ethylene) (PE). a) Rigid crystalline and mobile amorphous domains form sandwich structures with a period of the order of 20 nm. They are separated by narrow interfacial regions with intermediate mobility. b) Microscope image of an electrical tree in PE. The tree consists of a root-like system from about 10^5 cavities with typical diameters of 5 µm which are produced by electrical discharges. The pencil-like tip of the needle electrode is recognized above the tree.

MOUSE (MObile Universal Surface Explorer) has been developed[10-12]. This can be applied to arbitrarily large objects for NMR analysis of near-surface volume elements. Contrary to conventional NMR, the presence of ferromagnetic components is not necessarily detrimental, so that, for example, steel-belted car tires can be investigated. Good correlations have been found between NMR parameters measured with the NMR-MOUSE and many material parameters, for example the glass transition temperatures of a series of unfilled SBR samples with different cross-link densities.

Electrical Treeing in Poly(ethylene)

Poly(ethylene) (PE) is a semicrystalline material, in which crystalline lamellae and amorphous material are arranged in sandwich structures (Fig. 1a), which, on a larger scale, form spherulitic crystal structures[13]. An interfacial region of intermediate mobility with respect to the mobile amorphous and rigid crystalline domains can be detected by NMR. These structures are perturbed by the formation of electrical trees (Fig. 1b), which are collections of small cavities produced by electrical discharges. They are the manifestation of a major form of failure of polymeric insulation material in underground high-voltage cables[14,15]. Slightly cross-linked LDPE (low density PE) is a typical high-voltage cable insulation material and its electrical aging characteristics are the subject of extensive investigations. Typical testing arrangements are a needle-plate geometry, where an approximately cubic sample of PE with dimensions $(15\ mm)^3$ is positioned on a plate electrode and a needle with a well-defined radius is pressed into the sample. An alternating voltage is subsequently applied between needle and plate and slowly increased to about 40 kV. During this process some 10^5 discharges can be recorded until the insulating property of

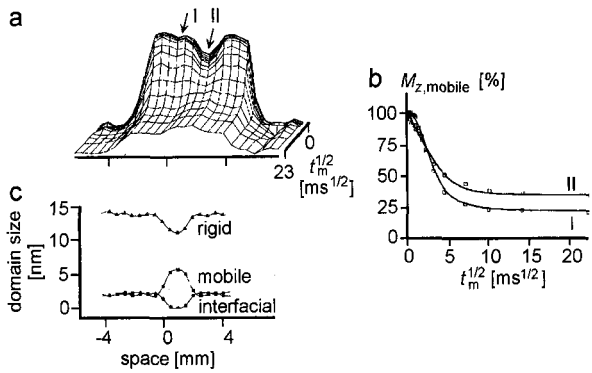

Fig. 2: Spin diffusion in LDPE. a) Spin-diffusion curves showing the decay of magnetization in the mobile chain segments as a function of distance across the sample. The symbols I and II mark the regions unaffected and affected by the electrical aging process, respectively.
b) Representative magnetization decays from regions I and II. Their different shapes indicate different morphologies. Dots: Experimental values. Solid lines: Simulations. c) 1D parameter images of domain sizes obtained from fits of spin diffusion curves in a model structure to the experimental curves for each pixel. Notable changes in the domain sizes are observed in the damaged part compared to the unaffected part.

the material has been destroyed by current breakthrough. Each discharge creates a small cavity. These cavities are connected and form a tree-like structure.

The average morphology of the sample is accessible from analysis of NMR spin-diffusion curves. Here spin diffusion denotes the migration of nuclear magnetization through the sample. It can be followed by dedicated experiments, after an initial non-equilibrium state of nuclear polarization has been established for instance, by localizing the nuclear polarization in the mobile amorphous domains only[16, 17]. By recording the migration of magnetization from the mobile domains to the rigid domains in terms of spin-diffusion, the average dimensions of domains with rigid, intermediate and mobile molecular segments can be derived by fitting theoretical spin-diffusion curves for a model of the polymer morphology to the experimental curves for each pixel.

Sample geometry and experimental results from 1D spin-diffusion imaging on electrically aged polyethylene[8,9] are summarized in Fig. 2. Region I marks the unaffected material and region II the location of the tree. The amplitudes of the magnetization decays are weighted by the spin-density values (a). A reduced value of the spin density in region II is explained by the presence of an electrical breakthrough channel and by a little hole from the needle electrode, which had been removed before measurement. Representative magnetization decays of both regions are compared in (b) after normalization to the same amplitude. The dots represent experimental values, and the solid lines are simulated decays. The decay in region I starts

with a plateau and is curved, while the decay in region II is initially linear. The length of the initial plateau defines the time delay for the magnetization to leave the mobile domains while the rigid domains are being magnetized from the domains with intermediate mobility. Thus the plateau indicates the presence of an interface. Lack of a plateau in the spin diffusion curves of regions II point to a negligibly thin interface.

1D parameter images of the dimensions of amorphous, crystalline and interfacial domains in the electrically aged LDPE sample are depicted in Fig. 2c. A variation of the domain sizes is clearly visible across the electrically aged region. The size of the rigid domains decreases from values of about 13.8 to 11.2 nm, that of the interface decreases from about 2.4 nm to 0.2 nm, while the size of the mobile domains increases from about 2 nm to 5.8 nm. The long period obtained from the fits is in reasonable agreement with the long period determined by small-angle X-ray scattering and is reduced by about 15 % in the affected region. Such a small change is more difficult to detect by X-ray scattering than a change of the order of 100 % by NMR in the dimension of the interfacial region. The change in morphology is interpreted to result from rapid local heating and subsequent rapid heat dissipation during formation of the tree with each electrical discharge. This interpretation explains the increase in diameter of the amorphous domains at the expense of that of the crystalline domains. The apparent loss of the interface points to the limits of the model used for analysis. It is likely, that the flat sheet structure of the sandwich layer model of PE needs to be replaced by one with a rough or fractal structure of the interface between rigid and mobile domains.

This example demonstrates the principal feasibility of imaging rigid polymers while addressing a question of general interest. Yet the experimental effort involved is considerable, and for reasons of radio-frequency power the samples need to be kept small. Therefore NMR imaging of rigid solids appears to be restricted to selected fundamental investigations.

Interfacial Layers in Covulcanized Rubber Sheets

Many elastomer products, in particular tires and conveyor belts are covulcanizates of different rubber compounds. Depending on the function of the rubber layer within the product, different formulations are used. Thus the rubber material itself and also the additives like filler, cross-linker, oil, etc. will vary in quality and quantity. During the vulcanization process the mobile components will show enhanced diffusion depending on the local temperature. This diffusion is hindered by the advancing vulcanization front. The competing interplay between diffusion of additives including rubber chains and sulfur may give rise to the formation of complex network structures which are superposed to the intended layer structure of the covulcanizate. This was observed first by NMR imaging of sections from a car tire at the interface between carbon-black filled styrene-co-butadiene and natural rubber[4]. The same

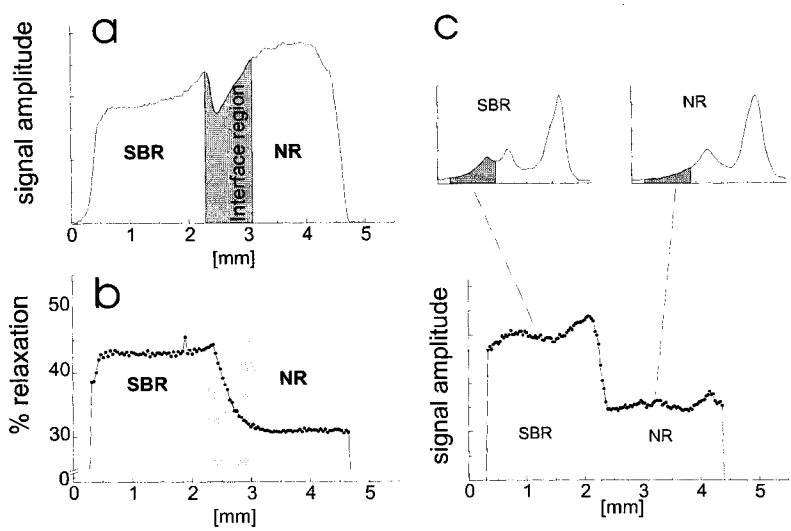

Fig.3: Spin-echo images of a covulcanizate from SBR and NR. a) 1D image. b) Ratio of two images with different relaxation weights. For comparison, the image has been overlaid to the spin-echo image *a*. c) 1D chemical-shift selective image of the aromatic CH signals. The area of integration is shaded in grey in the spectra of SBR and NR above. The thin line outlines the spin-echo image for comparison.

phenomenon has been observed later by visual inspection in covulcanizates from unfilled rubbers[18]. The stucture of the interface is a subject of on-going investigations by various analytical methods[5]. Similar phenomena have been observed in samples that were prepared by incomplete mixing of different components[19].

Results from NMR-imaging across the interface of two covulcanized sheets of SBR (styrene-butadiene rubber) and NR (nitrile rubber) are presented in Fig. 3. In this unfilled system an interfacial region could be detected already by inspection. In the 1D image, Fig. 3a, an interface is identified by a dip in the signal intensity. By forming the ratio, Fig. 3b, of two images with different relaxation weights, the spin density is eliminated, and the images contrast is a function of the relaxation time only. In this image no hints are found which indicate higher cross-link density in the region of the dip. For comparison, the spin-echo image 3a is shown in the background. Thus the dip is likely to be caused by a change in sulphur concentration. More detailed insight into the interface region is obtained by chemical-shift selective imaging of the magnetization from the aromatic CH signals. The respective area of integration are shaded in grey in the spectra of SBR and NR in 3c. In this region no peak but only a signal tail is detected in the NR spectrum. The chemical-shift selective image 3c clearly shows that the interface includes a region of interdiffusion between NR and SBR. The thin line outlines the spin-echo image for comparison. These measurements illustrate the

fine detail which can be obtained by NMR imaging on such a technologically important topic. A quantitative explanation of these effects needs to take into account the time-dependence of temperature, cross-link density and diffusion constants of different components across the sample during the curing process.

Cross-Filtration in Hollow-Fiber Membrane-Filter Modules

Filtration of liquids is a fundamental issue with important applications in chemical engineering, environmental science, and medicine.[20] Filtration membranes are made from different polymers, including poly(propylene) and cellulose material. They come in the form of sheets and hollow fibers. The type of membrane, their physical arrangement in the housing, and the operating conditions of a filter module determine the quality of the filtering process. However, not much about the details of the filtering process and the velocity distributions within the filter module is known, because noninvasive observations of material transport are limited to techniques using lasers light scattering or radioactive tracers unless NMR is employed.

During the last few years flow patterns and polarization-concentration patterns have been investigated by NMR in hollow-fiber membrane-filter modules[7,21-23]. Depending on the type of module, channeling of the feedstock flow may arise, which can significantly affect the operation efficiency. A more subtle issue is the direct measurement of molecules crossing the membrane. Inside the hollow fiber, the fluid flows in one direction, outside of it in the opposite direction. Depending on the pressure drop an inversion point may be located within the module. Before the inversion point molecules cross the membrane from the fiber lumen to the outside, and beyond the inversion point, the direction of trans-membrane flow is reversed.

A functional analysis of a membrane-filter module with respect to trans-membrane filtration is hampered by the low intensity of the trans-membrane flow. In principle a velocity-exchange experiment would be suitable, which correlates a particle displacement during a fixed interval at time t_1 with a particle displacement during another interval of the same duration at time t_2 some time t_m later[24,25]. In the terminology of exchange NMR, the velocity exchange spectrum provides the conditional probability that a molecule having velocity v_1 at time t_1 has a velocity v_2 at time t_2 a fixed time t_m later. For investigations of trans-membrane filtration one is interested in those molecules, which change direction during t_m, because these are the molecules which must have crossed the membrane. From the 2D exchange spectrum covering positive and negative axial flow, the respective signals will be found in the off-diagonal quadrants (Fig. 4a). The peak amplitude will be spread over this quadrant and will depend on the number of spins changing direction within the sensitive

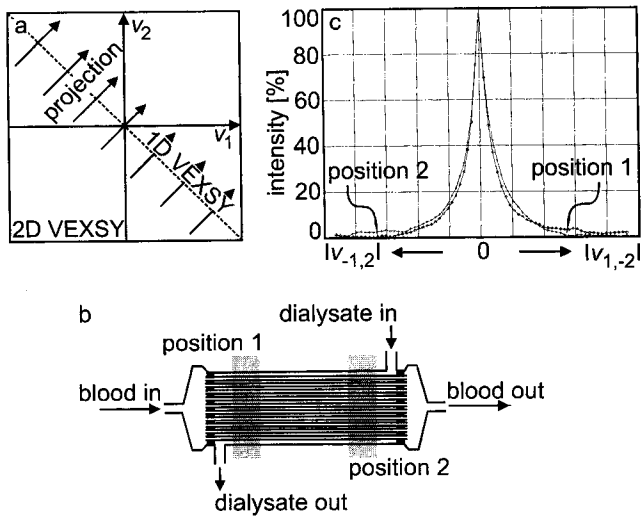

Fig. 4: Velocity exchange NMR. a) Schematic drawing of the experiment. v_1 is the initial velocity of a molecule and v_2 is the final velocity after the exchange time t_m. In the present case both velocities are in axial direction of the filtration module. The direction of integration for obtaining the 1D projection discussed in the text is indicated by arrows. b) Hollow-fiber membrane-filter module. Within and outside the hollow fibers the liquids flow in opposite directions. The positions for measurement of the velocity exchange projections are indicated. c) Velocity exchange projections measured at both positions of the filter module.

volume during the experiment. To increase this peak amplitude and thus to increase sensitivity, the 2D exchange spectrum should be integrated over the direction parallel to the diagonal, that is, a projection onto the subdiagonal should be calculated. Since the exchange spectrum is obtained by 2D Fourier transformation of a data set measured in the Fourier domain, the formation of the projection can be replaced by measurement of a slice in the Fourier domain. Therefore, acquisition of the projection of the velocity exchange experiment can be done in 6 min instead of at least 1 h of measurement time for a complete 2D exchange spectrum.

This experiment has been performed on a model dialysis module with suitably adjusted operating conditions, so that the inversion point was located somewhere in the middle of the module (Fig. 4b)[26]. One projection has been measured with the resonator for the NMR experiment at one end of the module, and another one with the resonator at the other end. The resultant projections are illustrated in Fig. 4c. Both projections show strong signals in the center, corresponding to the molecules which have not changed their direction of flow. But to the right and to the left a slightly but clearly elevated signal can be found. For the projection measured at the entrance of the module the elevated signal is at the right, corresponding to an exchange of flow from inside the hollow fiber in the positive direction to flow outside the

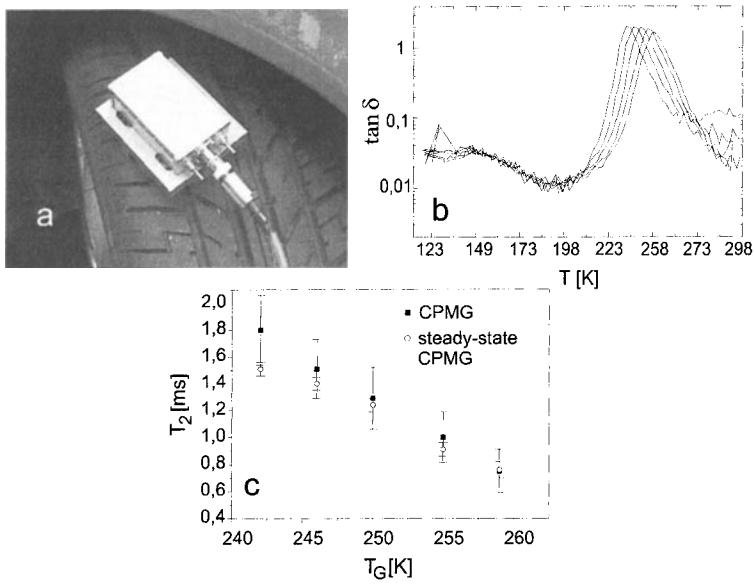

Fig. 5: The NMR-MOUSE. a) Use of the NMR-MOUSE for *in situ* measurements on a car tire. b) Determination of the glass transition temperature for a cross-link series of unfilled SBR samples: Phase shift tan δ from dynamic mechanical measurements as a function of temperature. c) Glass transition temperature T_g from the peak of the tan δ curve versus transverse relaxation time by the NMR-MOUSE measured by two different methods (CPMG and steady-state CPMG); CPMG = Carr Purcell Meiboom Gill pulse sequence.

fiber in the negative direction. The projection measured at the other end of the module exhibits an elevated signal at the other side of the central peak, indicating an exchange of velocity from negative to positive values. Thus despite its inherently low sensitivity, NMR can be used to investigate trans-membrane filtration, provided that suitable experiments are available. The velocity exchange experiment presented here is not an imaging experiment, but it has been applied in a spatially selective fashion to the object.

The NMR-MOUSE

The most important contrast parameters for discrimination of material properties in imaging are relaxation times[3]. In contrast to spectroscopic analysis no homogeneous magnetic fields are required for measurement of relaxation times. Thus single-sided application of inhomogeneous magnetic fields to large objects is feasible for discrimination of material properties by NMR[27]. The NMR-MOUSE is a novel NMR detector which has been developed for materials analysis in quality and process control[10]. A fist-size probe provides both, the polarizing magnetic field $\boldsymbol{B}_0$ from permanent magnets and the rf field from a surface coil (Fig. 5a). Magnetization build-up and decay curves can be measured by a variety of

techniques, including multi-echo techniques for averaging of spin interactions in solids[12]. Because of strong gradients in the polarizing $\boldsymbol{B}_0$ magnetic field (10 to 15 T/m) translational diffusion can be measured as well, and the liquid-state NMR signal is efficiently suppressed in emulsions and suspensions[28]. Even the presence of ferromagnetic objects is not necessarily an obstacle to the NMR-MOUSE: Material change from weathering could be identified by changes in T_2 of a 0.5 mm thick PVC coating of a 1 mm thick sheet of iron[11].

In elastomers the transverse magnetization decay can be used to characterize cross-link density, stress and temperature. The features of this approach are demonstrated in Fig. 5b) by relaxation times acquired with the NMR-MOUSE at room temperature for a series for differently cross-linked elastomer samples. The NMR data are plotted against the glass transition temperature, which has been determined from the maximum of the loss modulus by temperature dependent measurements on specially prepared test samples. It is important to note, that the MOUSE measurements can be performed on arbitrarily large samples in a nondestructive fashion, but that depth and size of the sensitive volume scale with the size of the coil of the NMR-MOUSE. In general, the larger the coil, the deeper the signal-bearing volume. Typical penetration depth are 1 to 3 mm with measurement times of the order of 1 to 15 minutes. The sensitive volume of the prototype MOUSE is equal approximately to the volume of a dime. Scanning of depth is achieved by changing the excitation and detection frequency, and lateral resolution is obtained by displacement of the scanner.

This example demonstrates, that spatially resolved NMR benefits not only from the development of new NMR methods, but also from new NMR hardware. In fact the NMR-MOUSE is a comparatively inexpensive NMR instrument well suited for a variety of potential applications in process and quality control from polymers to food stuffs and applications in medicine.

Summary

An overview of recent applications of spatially resolved NMR for testing properties and function of polymer materials has been given. Examples were selected to illustrate the analysis of properties from solid polymers and soft materials like elastomers by NMR imaging techniques as well as by a specially developed, new instrument, the NMR-MOUSE. A functional analysis of a hollow-fiber filtration module was reported by measuring localized projections of 2D velocity exchange spectra. A conceptually similar approach is followed by the NMR-MOUSE, where localized relaxation measurements are performed near the surface of objects, which can be made *in situ* for process and quality control.

Acknowledgement

This work has been supported by the Deutsche Forschungsgesellschaft (DFG, Bl 231/17-1 and Zi 505/1-1).

References

[1] P. Blümler, B. Blümich, R. Botto, E. Fukushima, *Spatially Resolved Magnetic Resonance*, VCH-Wiley, Weinheim 1998

[2] B. Blümich, W. Kuhn, *Magnetic Resonance Microscopy: Methods and Applications in Materials Science, Agriculture and Biomedicine*, VCH, Weinheim 1992

[3] B. Blümich, *Concepts Magn. Reson.* **10**, 19 (1998)

[4] P. Blümler, B. Blümich, H. Dumler, *Kautschuk, Gummi, Kunststoffe* **45**, 699 (1992)

[5] K. Unseld, private communication

[6] P. T. Callaghan, *Principles of Magnetic Resonance Mircoscopy*, Clarendon Press, Oxford 1991

[7] S. Laukemper-Ostendorf, H. D. Lemke, P. Blümler, B, Blümich, *J. Membrane Science* **138**, 287 (1998)

[8] F. Weigand, H. W. Spiess, B. Blümich, G. Salge, K. Möller, *IEEE Trans. Dielec. Elec. Insul.* **4**, 280 (1997)

[9] F. Weigand, D. E. Demco, B. Blümich, H. W. Spiess, *J. Magn. Reson.* **A 120**, 190 (1996)

[10] G. Eidmann, R. Savelsberg, P. Blümler, B. Blümich, *J. Magn. Reson.* **A 122**, 104 (1996)

[11] A. Guthausen, G. Zimmer, P. Blümler, B. Blümich, *J. Magn. Reson.* **130**, 1 (1998)

[12] G. Zimmer, A. Guthausen, U. Schmitz, K. Saito, B. Blümich, *Advanced Materials* **9**, 987 (1997)

[13] H.-G. Elias, *Makromoleküle*, vol. 1, 5th edition, Hütig & Wepf, Basel 1990

[14] R. J. Densley, *IEEE Trans. Electrical Insulation* **EI-14,** 148 (1979)

[15] E. J. McHahon, *IEEE Trans. Electrical Insulation* **EI-13,** 277 (1978)

[16] K. Schmidt-Rohr, H. W. Spiess, *Multidimensional Solid-State NMR and Polymers*, Academic Press, London 1994

[17] D. E. Demco, A. Johanson, J. Tegenfeldt, *Solid State Nucl. Magn. Reson.* **4,** 13 (1995)

[18] C. Fülber, *NMR-Relaxation und Bildgebung an Kautschuknetzwerken*, Akademischer Verlag, München 1996.

[19] P. Blümler, V. Litvinov, H. G. Dickland, M. van Duin, *Kautschuk, Gummi, Kunststoffe*, in press, (1998

[20] M. R. Kula, K. Schügerl, C. Wardrey, eds., *Technische Membranen in der Biotechnologie*, VCH, Weinheim 1986

[21] J. M. Pope, S. Yao, A.G. Fane, *J. Membr. Sci.* **118**, 247(1996)

[22] Yao, A. G. Fane, J. M. Pope, *Magn. Res. Imag.* **12**, 235 (1997)

[23] Yao, M. Costello. A.G. Fane, J. M. Pope, *J. Membr. Sci.* **99**, 207 (1995)

[24] P. T. Callaghan, B. Manz, *J. Magn. Reson.* **A 106**, 260 (1994)

[25] J. D. Seymour, P. T. Callaghan, *AICHE J.* **43**, 2096 (1997)

[26] V. Göbbels, B. Blümich, manuscript in preparation

[27] G. A. Mazkanin, in: P. Höller, V. Hauck, C. O. Rund, R. E. Green, eds., *Nondestructive Characterization of Materials*, Springer, Berlin 1989

[28] G. Zimmer, A. Guthausen, R. Eymael, B. Blümich, manuscript in preparation